

## Transformation of Finite Olver-Gaussian Beams by an Uniaxial Crystal Orthogonal to the Optical Axis

Salima Hennani, Lahcen Ez-Zariy\*, and Abdelmajid Belafhal

**Abstract**—The properties of the Finite Olver-Gaussian beams propagating through an uniaxial crystal orthogonal to the optical axis are studied. An analytical expression is developed, and some numerical simulations are performed to investigate the effects of some parameters on intensity distribution and profile of this beams family at the out-put plane of the uniaxial crystal. The results show that the beam exiting the optical system depends on the ratio of the extraordinary refractive index to the ordinary refractive index. Upon propagation in the uniaxial crystal, the Finite Olver-Gaussian beam in two transversal directions accelerates, while the acceleration in the transversal direction orthogonal to the optical axis is far slower than that in the transversal direction along the optical axis.

### 1. INTRODUCTION

It is known that during the last few decades, the transformation of a laser beam by an anisotropic medium was offered [1, 2]. Authors have shown that a relatively high-power beam through an anisotropic medium changes its structure during propagation with a nonlinear response of the permittivity. Just recently, Konar et al. [3–5] have studied a nonlinear evolution of non-Gaussian lasers beams in nonlinear media.

The propagation of laser beams through an anisotropic medium such as uniaxial crystals is derived by solving Maxwell's equations. This method is based on the fact that the optical field inside an anisotropic medium can be evaluated as a superposition of ordinary and extraordinary beams [6, 7]. The theoretical approach to describe the paraxial propagation of laser beam along the optical axis of an uniaxial medium is introduced for the first time by Ciattoni et al. [8–10]. Subsequently, they have introduced the paraxial and non-paraxial approaches to characterize a laser beam propagating an uniaxial crystal orthogonal to the optical axis [11–13]. After these, a lot of studies elaborated in the context have treated the propagation of laser beams through an uniaxial crystal orthogonal to the propagation axis. Liu and Zhou [14] have examined the case of dark hollow beams passing through uniaxial crystals orthogonal to the optical axis. Tang [15] has analyzed a linearly polarized Hermite-cosine-Gaussian, and the propagation properties of Lorentz and Lorentz-Gaussian beams through the same optical system have been researched by Gawhary and Li [16, 17]. The propagation of phase-locked and non-phase-locked Gaussian array beams in the considered system is investigated by Liu and Zhao [18]. Parallel with this, another study in the same optic was made on the confluent hypergeometric beams by Li and Chen [19]. Recently, the analytical expression of the propagation of an Airy beam in uniaxial crystals is devoted by Zhou et al. [20]. However, to the best of our knowledge, so far, there have no reference reporting the propagation properties of Finite Olver-Gaussian beams through uniaxial crystals orthogonal to the optical axis. This novel beams family which is demonstrated as a solution of Olver's differential equation [21], is considered as a special generalization of Airy beams.

---

*Received 24 October 2015, Accepted 18 December 2015, Scheduled 4 January 2016*

\* Corresponding author: Lahcen Ez-Zariy (ezzariy@gmail.com).

The authors are with the Laboratory of Nuclear, Atomic and Molecular Physics, Department of Physics, Faculty of Sciences, Chouaib Doukkali University, P. B 20, 24000 El Jadida, Morocco.

In the present work, the diffraction field components of Finite Olver-Gaussian beams are studied by numerical examples. The influence of beam parameters together with the ratio of refractive indices of uniaxial crystals on extraordinary polarized beams are discussed. In Section 2, analytical formulas for the propagation of the uniaxial crystal are derived. In Section 3, the propagation properties of the Finite Olver-Gaussian beams are illustrated by numerical examples. Finally, some conclusions are outlined in Section 4.

## 2. PROPAGATION OF FINITE OLVER-GAUSSIAN BEAMS IN UNIAXIAL CRYSTAL

Consider a lossless uniaxial crystal whose optical axis coincides with the  $x$ -axis, whereas the light beam propagates along the  $z$ -axis. In this frame of reference, the relative dielectric tensor reads as [11]

$$\varepsilon = \begin{pmatrix} n_e^2 & 0 & 0 \\ 0 & n_0^2 & 0 \\ 0 & 0 & n_0^2 \end{pmatrix}, \quad (1)$$

where  $n_e$  and  $n_0$  are the extraordinary and ordinary refractive indexes, respectively. Assume that a Finite Olver-Gaussian beam linearly polarized in  $x$ -direction illuminates an uniaxial crystal in the plane ( $z = 0$ ) and propagates toward the half space ( $z > 0$ ). The initial polarized Finite Olver-Gaussian beam at the source plane ( $z = 0$ ) takes the form [21]

$$\begin{bmatrix} E_x(x_0, y_0, 0) \\ E_y(x_0, y_0, 0) \end{bmatrix} = \begin{bmatrix} O_n\left(\frac{x_0}{\omega_0}\right) O_n\left(\frac{y_0}{\omega_0}\right) \exp\left\{\frac{a}{\omega_0}(x_0 + y_0)\right\} \exp\left\{\frac{-b}{\omega_0^2}(x_0^2 + y_0^2)\right\} \\ 0 \end{bmatrix}, \quad (2)$$

where  $\omega_0$  is the transverse scale,  $a$  the modulation parameter and  $b$  a Gaussian parameter to be equal to 0 or 1.  $O_n(\cdot)$  is the Olver function of order  $n = 0; 1; 2; \dots$ , and its integral representation is given by

$$O_n(x) = \frac{1}{2\pi} \int_{-\infty}^{+\infty} \exp(c(it)^\gamma + itx) dt, \quad (3)$$

with  $\begin{cases} \gamma = n + 3, \\ |c| = \frac{1}{n+3}. \end{cases}$

Within the accuracy of the paraxial approximation, the propagation electrical field components of electromagnetic beams passing through uniaxial crystals orthogonal to the optical axis has been evaluated by the following integrals [11, 20]

$$E_x(x, y, z) = \exp\{ikn_e z\} \int_{-\infty}^{+\infty} \int_{-\infty}^{+\infty} \bar{E}_x(k_x, k_y) \exp\left\{i(k_x x + k_y y) - i\frac{n_e^2 k_x^2 + n_0^2 k_y^2}{2kn_0^2 n_e} z\right\} dk_x dk_y, \quad (4)$$

$$E_y(x, y, z) = \exp\{ikn_0 z\} \int_{-\infty}^{+\infty} \int_{-\infty}^{+\infty} \bar{E}_y(k_x, k_y) \exp\left\{i(k_x x + k_y y) - i\frac{k_x^2 + k_y^2}{2kn_0} z\right\} dk_x dk_y, \quad (5)$$

with

$$\bar{E}_j(k_x, k_y) = \frac{1}{(2\pi)^2} \int_{-\infty}^{+\infty} \int_{-\infty}^{+\infty} E_j(x_0, y_0, z=0) \exp\{-i(k_x x_0 + k_y y_0)\} dx_0 dy_0; \quad j = x, y \quad (6)$$

is the two-dimensional Fourier transform of  $x$ - and  $y$ -transverse Cartesian components of the initial electrical field at the plane ( $z = 0$ ). These components can be considered as a superposition of

extraordinary waves for the  $x$ -component and  $y$ -component contains ordinary plane waves [16]. Equations (5) and (6) can also be rewritten respectively as [19]

$$E_x(x, y, z) = \frac{kn_0}{2\pi iz} \exp\{ikn_e z\} \int_{-\infty}^{+\infty} \int_{-\infty}^{+\infty} E_x(x_0, y_0, 0) \exp\left\{i \frac{k}{2zn_e} [n_0^2 (x - x_0)^2 + n_e^2 (y - y_0)^2]\right\} dx_0 dy_0, \quad (7)$$

$$E_y(x, y, z) = \frac{kn_0}{2\pi iz} \exp\{ikn_0 z\} \int_{-\infty}^{+\infty} \int_{-\infty}^{+\infty} E_y(x_0, y_0, 0) \exp\left\{i \frac{kn_0}{2z} [(x - x_0)^2 + (y - y_0)^2]\right\} dx_0 dy_0, \quad (8)$$

where  $k = \frac{2\pi}{\lambda}$  denotes the wave number with  $\lambda$  the wavelength of the incident beam.  $\vec{k} = (k_x, k_y)$  represents the transverse wavelength vector evaluated in the frequency domain. Substituting Eq. (2) into Eqs. (7) and (8), one obtains

$$E_x(x, y, z) = \frac{kn_0}{2\pi iz} \exp\{ikn_e z\} U(x, z) U(y, z), \quad (9)$$

with

$$U(x, z) = \int_{-\infty}^{+\infty} O_n\left(\frac{x_0}{\omega_0}\right) \exp\left\{-\frac{b}{\omega_0^2} x_0^2 + \frac{a}{\omega_0} x_0\right\} \exp\left\{-\frac{kn_0^2}{2izn_e} (x - x_0)^2\right\} dx_0, \quad (10)$$

and

$$U(y, z) = \int_{-\infty}^{+\infty} O_n\left(\frac{y_0}{\omega_0}\right) \exp\left\{-\frac{b}{\omega_0^2} y_0^2 + \frac{a}{\omega_0} y_0\right\} \exp\left\{-\frac{kn_e}{2iz} (y - y_0)^2\right\} dy_0. \quad (11)$$

Eq. (10) can be rewritten as

$$U(x, z) = \exp\left\{-\frac{kn_0^2}{2izn_e} x^2\right\} \int_{-\infty}^{+\infty} O_n\left(\frac{x_0}{\omega_0}\right) \exp\left\{-\left(\frac{b}{\omega_0^2} + \frac{kn_0^2}{2izn_e}\right) x_0^2 + \left(\frac{a}{\omega_0} + \frac{kn_0^2}{izn_e} x\right) x_0\right\} dx_0. \quad (12)$$

By exploiting Eq. (3)

$$U(x, z) = \frac{1}{2\pi} \exp\left\{-\frac{kn_0^2}{2izn_e} x^2\right\} \int_{-\infty}^{+\infty} dt \exp\{c(it)^{n+3}\} \int_{-\infty}^{+\infty} \exp\left\{-\left(\frac{b}{\omega_0^2} + \frac{kn_0^2}{2izn_e}\right) x_0^2 + \left(\frac{a}{\omega_0} + \frac{kn_0^2}{izn_e} x + \frac{it}{\omega_0}\right) x_0\right\} dx_0, \quad (13)$$

by using the following integral formula [21, 22]

$$\int_{-\infty}^{+\infty} \exp(-p^2 x^2 \pm qx) dx = \frac{\sqrt{\pi}}{p} \exp\left\{\frac{q^2}{4p^2}\right\}, \quad (14)$$

with  $\text{Re}\{P^2 > 0\}$  and the expression [21]

$$\frac{1}{2\pi} \int_{-\infty}^{+\infty} \exp\left[c(iu)^{n+3} - \frac{1}{2} su^2 + iux\right] du = \exp\left\{\frac{s^3}{12} + \frac{sx}{2}\right\} O_n\left[x + \frac{s^2}{4}\right], \quad (15)$$

Eq. (12) turns out to be

$$\begin{aligned}
 U(x, z) = & \left( \frac{\pi}{\frac{b}{\omega_0^2} + \frac{kn_0^2}{2izn_e}} \right)^{1/2} \exp \left\{ -\frac{kn_0^2}{2izn_e} x^2 \right\} \exp \left\{ \frac{\left( \frac{a}{\omega_0} + \frac{kn_0^2}{izn_e} x \right)^2}{4 \left( \frac{b}{\omega_0^2} + \frac{kn_0^2}{2izn_e} \right)} \right\} \exp \left\{ \frac{1}{96\omega_0^6 \left( \frac{b}{\omega_0^2} + \frac{kn_0^2}{2izn_e} \right)^3} \right\} \\
 & \times \exp \left\{ \frac{\left( \frac{a}{\omega_0} + \frac{kn_0^2}{izn_e} x \right)}{8\omega_0^3 \left( \frac{b}{\omega_0^2} + \frac{kn_0^2}{2izn_e} \right)^2} \right\} O_n \left[ \frac{\left( \frac{a}{\omega_0} + \frac{kn_0^2}{izn_e} x \right)}{2\omega_0 \left( \frac{b}{\omega_0^2} + \frac{kn_0^2}{2izn_e} \right)} + \frac{1}{16\omega_0^4 \left( \frac{b}{\omega_0^2} + \frac{kn_0^2}{2izn_e} \right)^2} \right]. \quad (16)
 \end{aligned}$$

Using the same steps as before we find the following expression

$$\begin{aligned}
 U(y, z) = & \left( \frac{\pi}{\frac{b}{\omega_0^2} + \frac{kn_e}{2iz}} \right)^{1/2} \exp \left\{ -\frac{kn_e}{2iz} y^2 \right\} \exp \left\{ \frac{\left( \frac{a}{\omega_0} + \frac{kn_e}{iz} y \right)^2}{4 \left( \frac{b}{\omega_0^2} + \frac{kn_e}{2iz} \right)} \right\} \exp \left\{ \frac{1}{96\omega_0^6 \left( \frac{b}{\omega_0^2} + \frac{kn_e}{2iz} \right)^3} \right\} \\
 & \times \exp \left\{ \frac{\left( \frac{a}{\omega_0} + \frac{kn_e}{iz} y \right)}{8\omega_0^3 \left( \frac{b}{\omega_0^2} + \frac{kn_e}{2iz} \right)^2} \right\} O_n \left[ \frac{\left( \frac{a}{\omega_0} + \frac{kn_e}{iz} y \right)}{2\omega_0 \left( \frac{b}{\omega_0^2} + \frac{kn_e}{2iz} \right)} + \frac{1}{16\omega_0^4 \left( \frac{b}{\omega_0^2} + \frac{kn_e}{2iz} \right)^2} \right]. \quad (17)
 \end{aligned}$$

The propagation electrical field components of Finite Olver-Gaussian beams through an uniaxial crystal at the output plane is expressed as

$$\begin{aligned}
 E_x(x, y, z) = & \frac{kn_0}{2\pi iz} \exp \{ ikn_e z \} \left( \frac{\pi}{\frac{b}{\omega_0^2} + \frac{kn_0^2}{2izn_e}} \right)^{1/2} \left( \frac{\pi}{\frac{b}{\omega_0^2} + \frac{kn_e}{2iz}} \right)^{1/2} \\
 & \times \exp \left\{ -\frac{kn_0^2}{2izn_e} x^2 - \frac{kn_e}{2iz} y^2 \right\} \exp \left\{ \frac{\left( \frac{a}{\omega_0} + \frac{kn_0^2}{izn_e} x \right)^2}{4 \left( \frac{b}{\omega_0^2} + \frac{kn_0^2}{2izn_e} \right)} + \frac{\left( \frac{a}{\omega_0} + \frac{kn_e}{iz} y \right)^2}{4 \left( \frac{b}{\omega_0^2} + \frac{kn_e}{2iz} \right)} \right\} \\
 & \times \exp \left\{ \frac{1}{96\omega_0^6 \left( \frac{b}{\omega_0^2} + \frac{kn_0^2}{2izn_e} \right)^3} + \frac{\left( \frac{a}{\omega_0} + \frac{kn_0^2}{izn_e} x \right)}{8\omega_0^3 \left( \frac{b}{\omega_0^2} + \frac{kn_0^2}{2izn_e} \right)^2} \right\} \exp \left\{ \frac{1}{96\omega_0^6 \left( \frac{b}{\omega_0^2} + \frac{kn_e}{2iz} \right)^3} + \frac{\left( \frac{a}{\omega_0} + \frac{kn_e}{iz} y \right)}{8\omega_0^3 \left( \frac{b}{\omega_0^2} + \frac{kn_e}{2iz} \right)^2} \right\} \\
 & \times O_n \left[ \frac{\left( \frac{a}{\omega_0} + \frac{kn_0^2}{izn_e} x \right)}{2\omega_0 \left( \frac{b}{\omega_0^2} + \frac{kn_0^2}{2izn_e} \right)} + \frac{1}{16\omega_0^4 \left( \frac{b}{\omega_0^2} + \frac{kn_0^2}{2izn_e} \right)^2} \right] O_n \left[ \frac{\left( \frac{a}{\omega_0} + \frac{kn_e}{iz} y \right)}{2\omega_0 \left( \frac{b}{\omega_0^2} + \frac{kn_e}{2iz} \right)} + \frac{1}{16\omega_0^4 \left( \frac{b}{\omega_0^2} + \frac{kn_e}{2iz} \right)^2} \right]. \quad (18)
 \end{aligned}$$

From this last equation, one obtains the following propagation electrical field components of Finite

Olver beams ( $b = 0$ ) through uniaxial crystals at the output plane

$$E_x(x, y, z) = \exp\{ikn_e z\} \exp\left\{-\frac{kn_0^2}{2izn_e}x^2 - \frac{kn_e}{2iz}y^2\right\} \exp\left\{\frac{\left(\frac{a}{\omega_0} + \frac{kn_0^2}{izn_e}x\right)^2}{\left(\frac{2kn_0^2}{izn_e}\right)} + \frac{\left(\frac{a}{\omega_0} + \frac{kn_e}{iz}y\right)^2}{\left(\frac{2kn_e}{iz}\right)}\right\}$$

$$\times \exp\left\{\frac{2}{3}\left(\frac{izn_e}{\omega_0^2 kn_0^2}\right)^3 + \frac{\left(\frac{a}{\omega_0} + \frac{kn_0^2}{izn_e}x\right)}{\omega_0 \left(\frac{kn_0^2}{izn_e}\right)} \left(\frac{izn_e}{2\omega_0^2 kn_0^2}\right) + \frac{2}{3}\left(\frac{iz}{\omega_0^2 k}\right)^3 + \frac{\left(\frac{a}{\omega_0} + \frac{kn_e}{iz}y\right)}{\omega_0 \left(\frac{kn_e}{iz}\right)} \left(\frac{iz}{2\omega_0^2 kn_e}\right)\right\}$$

$$\times O_n \left[ \frac{\left(\frac{a}{\omega_0} + \frac{kn_0^2}{izn_e}x\right)}{\omega_0 \left(\frac{kn_0^2}{izn_e}\right)} + \left(\frac{izn_e}{2\omega_0^2 kn_0^2}\right)^2 \right] O_n \left[ \frac{\left(\frac{a}{\omega_0} + \frac{kn_e}{iz}y\right)}{\omega_0 \left(\frac{kn_e}{iz}\right)} + \left(\frac{iz}{2\omega_0^2 kn_e}\right)^2 \right], \quad (19)$$

$$E_y(x, y, z) = 0. \quad (20)$$

By the adoption of the notations:  $e = n_e/n_0$  the ratio of the extraordinary refractive index to the ordinary refractive index and  $z_0 = k\omega_0^2$ , one obtains

$$E_x(x, y, z) = \exp\{ikn_0 e z\} \exp\left\{\frac{a}{\omega_0}x - \frac{a}{2}\left(\frac{ze}{z_0 n_0}\right)^2 - \frac{i}{12}\left(\frac{ze}{z_0 n_0}\right)^3 + \left(a^2 + \frac{x}{\omega_0}\right)\left(\frac{ize}{2z_0 n_0}\right)\right\}$$

$$\times \exp\left\{\frac{a}{\omega_0}y - \frac{a}{2}\left(\frac{z}{z_0 n_0 e}\right)^2 - \frac{i}{12}\left(\frac{z}{z_0 n_0 e}\right)^3 + \left(a^2 + \frac{y}{\omega_0}\right)\left(\frac{iz}{2z_0 n_0 e}\right)\right\}$$

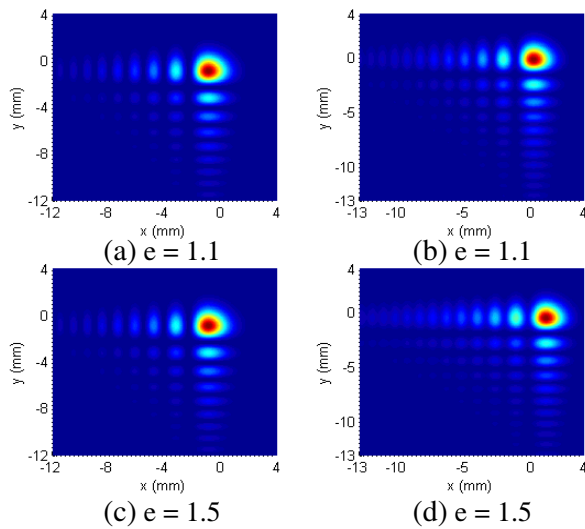


**Figure 1.** Contour graph of normalized intensity distribution of Finite Olver beam at  $n = 0$  propagating through uniaxial crystals orthogonal to the optical axis at different planes ((a), (c))  $z = z_0$  and ((b), (d))  $z = 5z_0$ . The top and bottom rows denote  $e = 1.1$  and  $e = 1.5$  respectively.

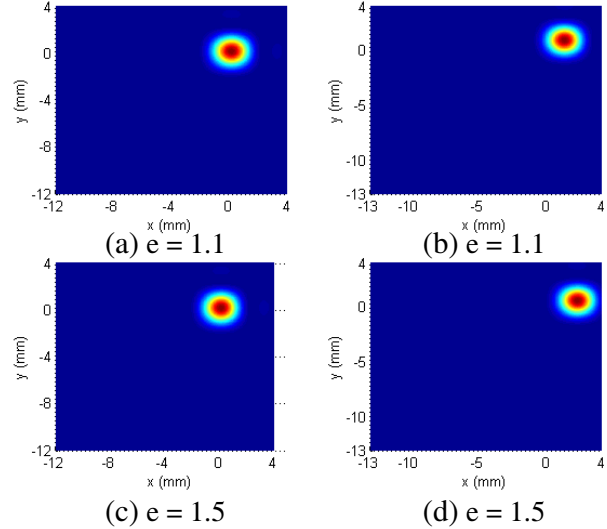


**Figure 2.** Contour graph of normalized intensity distribution of Finite Olver beam in first order ( $n = 1$ ) propagating through uniaxial crystals orthogonal to the optical axis at different planes ((a), (c))  $z = z_0$  and ((b), (d))  $z = 5z_0$ . The top and bottom rows denote  $e = 1.1$  and  $e = 1.5$  respectively.

$$\times O_n \left[ \frac{x}{\omega_0} - \left( \frac{ze}{2z_0 n_0} \right)^2 + \frac{iza e}{z_0 n_0} \right] O_n \left[ \frac{y}{\omega_0} - \left( \frac{z}{2z_0 e n_0} \right)^2 + \frac{iza}{z_0 n_0 e} \right], \quad (21)$$

$$E_y(x, y, z) = 0. \quad (22)$$

Finally, the resultant intensity distribution of the considered beams family propagating in uniaxial crystals at the distance can be approximately expressed as:  $I(x, y, z) = |E_x(x, y, z)|^2$ .

### 3. NUMERICAL RESULTS

In this section, we are interested in the numerical study of the propagation properties of the Finite Olver beams (without Gaussian term) through an uniaxial crystal orthogonal to the optical axis considering that  $b = 0$  and using the closed analytical expression established in Eq. (21). This choice is due to the dispersion of the secondary lobes of the Olver beams with the presence of the Gaussian modulation. The parameters used in calculations are chosen as  $\lambda = 0.53 \mu\text{m}$ ,  $\omega_0 = 100 \mu\text{m}$ ,  $a = 0.1$ , and  $n_0 = 2.616$ . The three observation planes are  $z = z_0$ ,  $z = 3z_0$ ,  $z = 5z_0$ . For all figures, the values of the normalized intensity distribution are of arbitrary unit (a.u.).

Figure 1 represents a contour graph of the normalized intensity distribution of ordinary Finite Olver beam ( $b = 0$ ) at  $n = 0$  which is a special case representing the shape of the Finite Airy beam, when the subscript means taking the maximum value. The top and bottom rows denote  $e = 1.1$  and  $e = 1.5$ ,

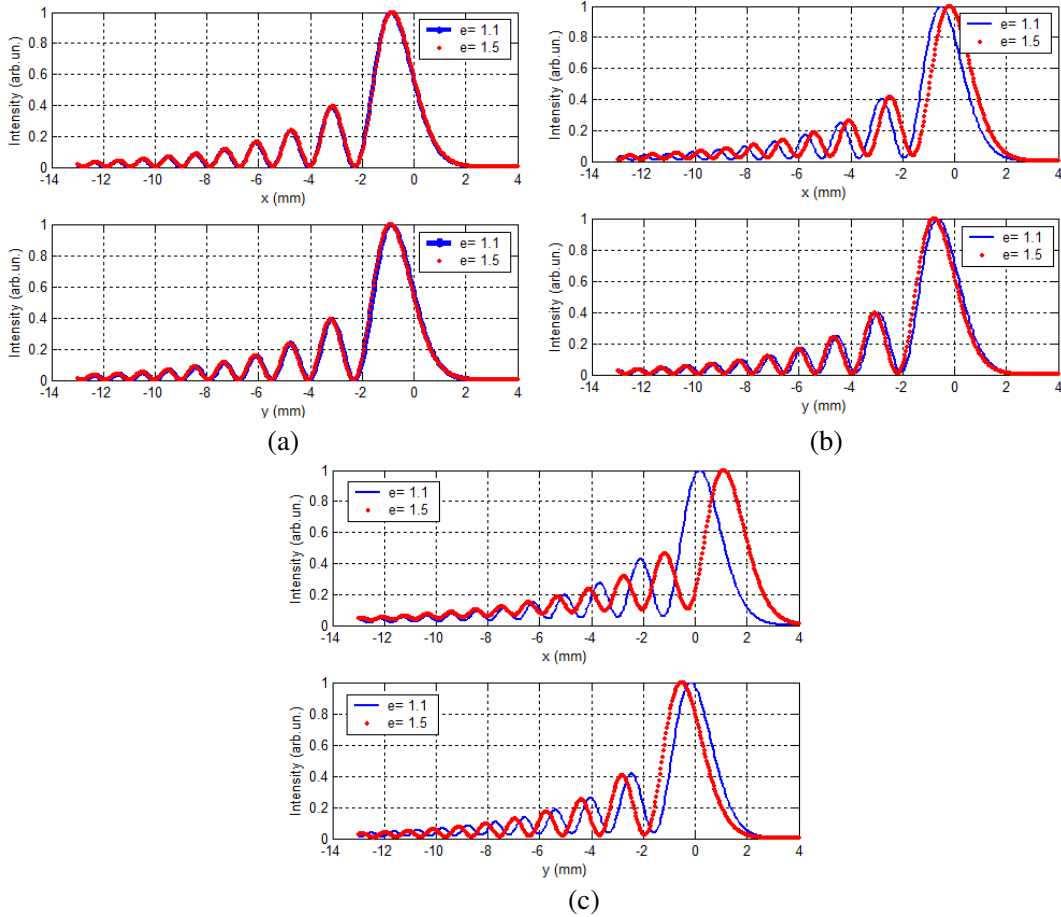


**Figure 3.** Intensity distribution in  $x$  direction and  $y$  direction of Finite Olver beams at  $n = 0$  propagating through uniaxial crystals orthogonal to the optical axis at different planes (a)  $z = z_0$ , (b)  $z = 3z_0$  and (c)  $z = 5z_0$ . The top and bottom rows denote  $e = 1.1$  and  $e = 1.5$  respectively.

respectively, with the two observation planes ((a), (c))  $z = z_0$  and ((b), (d))  $z = 5z_0$ . Fig. 2 depicts a contour graph of the normalized intensity distribution of Finite Olver beam of first order ( $n = 1$ ). The anisotropic effect of the crystals leads to an acceleration of the Finite Olver beam in  $y$ -direction slower than that in  $x$ -direction upon the propagation in the uniaxial crystals orthogonal to the optical axis. These results are compared with those given in [20].

In Figs. 3 and 4, we plot the acceleration properties of a Finite Olver beam for the two first orders  $n = 0$  and  $n = 1$  during propagation in  $x$  and  $y$  directions through uniaxial crystals. These figures confirm the remark obtained in Fig. 1, that the acceleration of Finite Olver beam is far faster in  $x$  direction than that in  $y$  direction with an increase in the value of the ratio  $e$ .

Figures 5 and 6 show contour graphs of the normalized intensity distribution of Finite Olver beam of the two first orders  $n = 0$  and  $n = 1$ , propagating through uniaxial crystals orthogonal to the optical axis at  $(z, x)$  and  $(z, y)$  planes. These draws are carried out in order to investigate the effects of the ratio  $e$  on the intensity of the Finite Olver observed at receiver plane of the uniaxial crystal. Still from these figures, it can be concluded that upon propagation in the uniaxial crystals, the Finite Olver beam in two transversal directions accelerates, while the acceleration in the transversal direction orthogonal to the optical axis is far slower than that in the transversal direction along the optical axis.

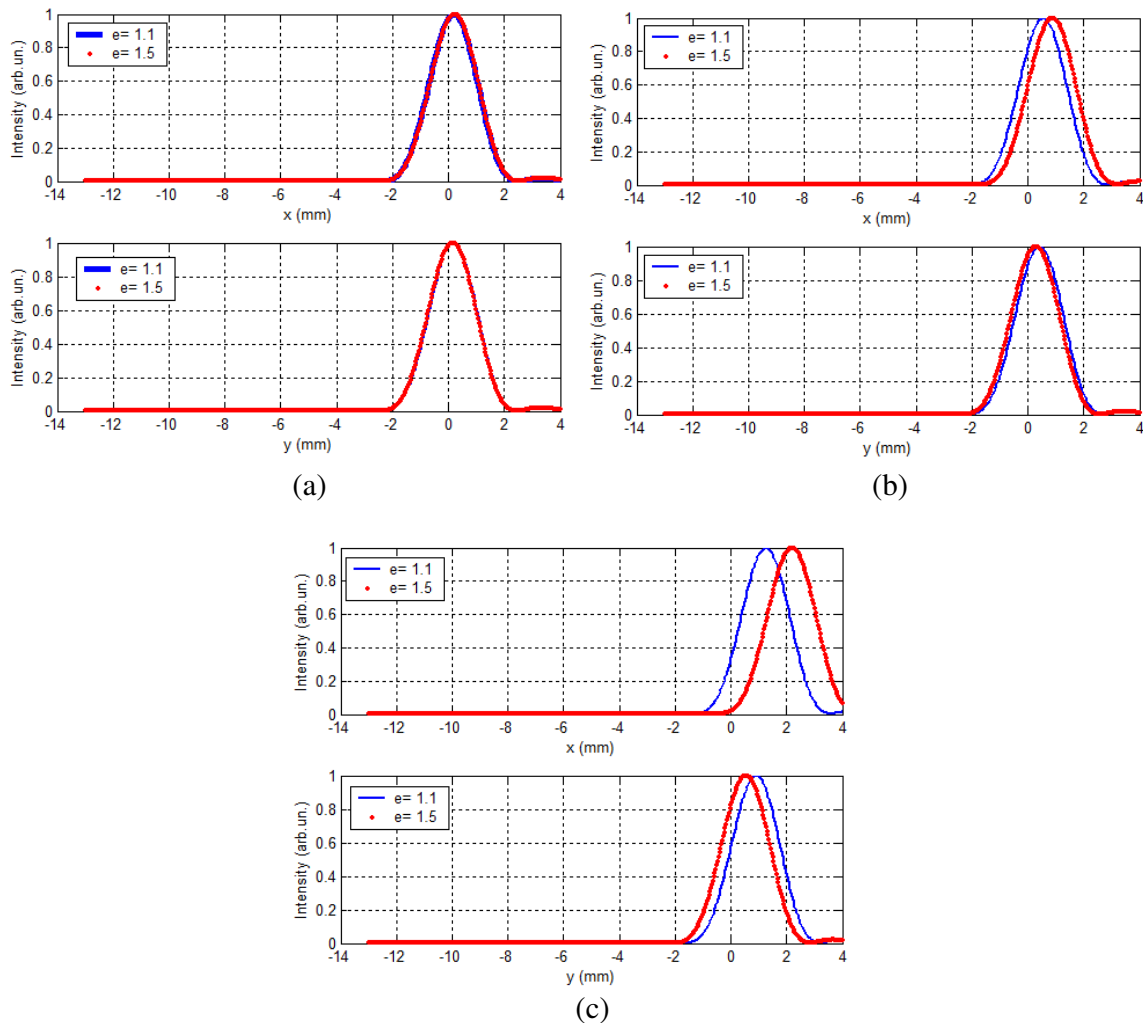


**Figure 4.** Intensity distribution in  $x$  direction and  $y$  direction of Finite Olver beam in first order at  $n = 1$  propagating through uniaxial crystals orthogonal to the optical axis at different planes (a)  $z = z_0$ , (b)  $z = 3z_0$  and (c)  $z = 5z_0$ . The top and bottom rows denote  $e = 1.1$  and  $e = 1.5$  respectively.

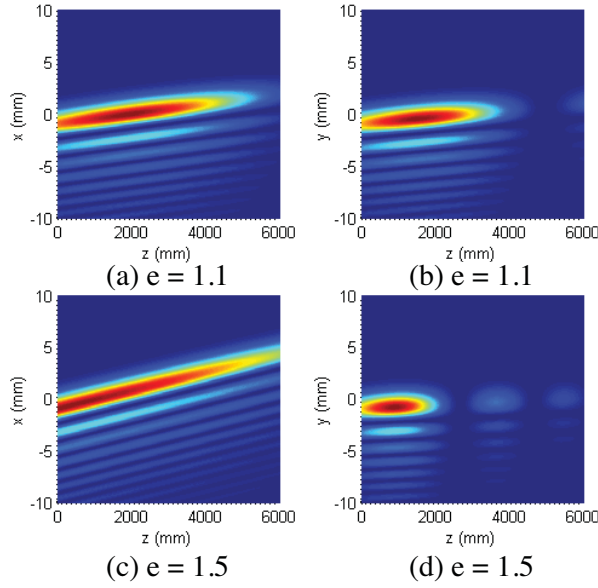


**Figure 5.** Contour graph of normalized intensity distribution of Finite Olver beam at  $n = 0$  propagating through uniaxial crystals orthogonal to the optical axis. ((a), (c))  $(x-z)$  plane and ((b), (d))  $(y-z)$  plane. The top and bottom rows denote  $e = 1.1$  and  $e = 1.5$  respectively.

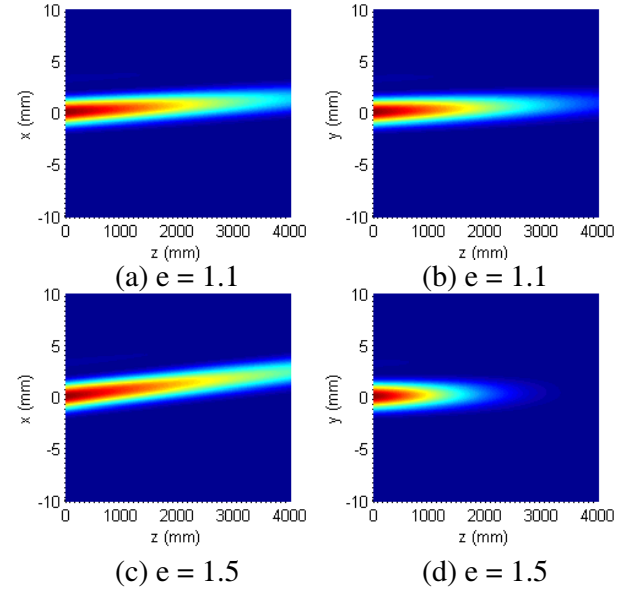


**Figure 6.** Contour graph of normalized intensity distribution of Finite Olver beam in first order at  $n = 1$  propagating through uniaxial crystals orthogonal to the optical axis. ((a), (c))  $(x-z)$  plane and ((b), (d))  $(y-z)$  plane. The top and bottom rows denote  $e = 1.1$  and  $e = 1.5$  respectively.

#### 4. CONCLUSION

Based on the theory of paraxial electromagnetic beams through uniaxial crystals orthogonal to the optical axis, we have derived the analytical formulas for Finite Olver-Gaussian and Finite Olver beams linearly polarized. The effects of the ordinary refractive  $n_o$ , ratio of the extraordinary refractive index to the ordinary refractive index  $e$ , axial propagation distance  $z$  and beam parameter  $\omega_0$  are analyzed and illustrated by numerical examples. The results show that as the case of the Airy beams, upon propagation through an uniaxial crystals, the Finite Olver-Gaussian beam spreads and accelerates in the transverse directions. These results may find their potential advantages in the usage of Finite OlverGaussian beams in anisotropic medium and trapping particles in nonlinear optical devices.

#### REFERENCES

1. Born, M. and E. Wolf, *Principles of Optics*, Oxford, Pergamon, UK, 1999.
2. Fleck, Jr., J. A. and M. D. Feit, "Beam propagation in uniaxial anisotropic media," *J. Opt. Soc. Am. A*, Vol. 73, 920–926, 1983.
3. Konar, S., M. Mishra, and S. Jana, "Nonlinear evolution of cosh-Gaussian laser beams and generation of flat top spatial solitons in cubic quintic nonlinear media," *Physics Letters A*, Vol. 362, 505–510, 2007.
4. Konar, S. and S. Jana, "Linear and nonlinear propagation of sinh-Gaussian pulses in dispersive media possessing Kerr nonlinearity," *Optics Communications*, Vol. 236, 7–20, 2004.
5. Jana, S. and S. Konar, "Tnable spectral switching in the far field with a chirped cosh-Gaussian pulse," *Optics Communications*, Vol. 267, 24–31, 2006.



6. Stamnes, J. J. and G. C. Sherman, "Radiation of electromagnetic fields in uniaxially anisotropic media," *J. Opt. Soc. Am.*, Vol. 66, 780–788, 1976.
7. Stamnes, J. J. and G. C. Sherman, "Radiation of electromagnetic fields in uniaxially anisotropic media," *J. Opt. Soc. Am.*, Vol. 68, 502–508, 1978.
8. Ciattoni, A. and C. Palma, "Ordinary and extraordinary beams characterization in uniaxially anisotropic crystals," *Optics Communications*, Vol. 195, 55–61, 2001.
9. Ciattoni, A., G. Cincotti, D. Provenziani, and C. Palma, "Paraxial propagation along the optical axis of a uniaxial medium," *Phys. Rev. E*, Vol. 66, 036614, 2002.
10. Ciattoni, A., G. Cincotti, and C. Palma, "Propagation of cylindrically symmetric fields in uniaxial crystals," *J. Opt. Soc. Am. A*, Vol. 19, 792–796, 2002.
11. Ciattoni, A. and C. Palma, "Optical propagation in uniaxial crystal orthogonal to the optical axis: Paraxial theory and beyond," *J. Opt. Soc. Am. A*, Vol. 20, 2163–2171, 2003.
12. Ciattoni, A. and C. Palma, "Nondiffracting beams in uniaxial media propagating orthogonally to the optical axis," *Optics Communications*, Vol. 224, 175–183, 2003.
13. Ciattoni, A., G. Cincotti, and C. Palma, "Laguerre-Gauss and Bessel-Gauss beams in uniaxial crystals," *J. Opt. Soc. Am. A*, Vol. 19, 1680–1688, 2002.
14. Liu, D. and Z. Zhou, "Various dark hollow beams propagating in uniaxial crystals orthogonal to the optical axis," *J. Opt. A: Pure Appl. Opt.*, Vol. 10, 095005, 2008.
15. Tang, B., "Hermite-cosine-Gaussian beams propagating in uniaxial crystals orthogonal to the optical axis," *J. Opt. Soc. Am. A*, Vol. 26, 2480–2487, 2009.
16. Gawhary, O. E. and S. Severini, "Lorentz beams and symmetry properties in paraxial optics," *J. Opt. A: Pure Appl. Opt.*, Vol. 8, 409–414, 2006.
17. Li, J., Y. Chen, S. Xu, Y. Wang, M. Zhou, Q. Zhao, Y. Xin, and F. Chen, "Propagation properties of Lorentz beam in uniaxial crystals orthogonal to the optical axis," *Opt. & Laser Tech.*, Vol. 43, 506–514, 2011.
18. Liu, Z. and D. Zhao, "Propagation of Gaussian array beams in uniaxial crystals orthogonal to the optical axis," *Optik*, Vol. 123, 208–211, 2012.
19. Li, J. and Y. Chen, "Propagation of confluent hypergeometric beam through uniaxial crystals orthogonal to the optical axis," *Opt. & Laser Tech.*, Vol. 44, 1603–1610, 2012.
20. Zhou, G., R. Chen, and X. Chu, "Propagation of Airy beams in uniaxial crystals orthogonal to the optical axis," *Opt. Exp.*, Vol. 20, 2196–2205, 2012.
21. Belafhal, A., L. Ez-zariy, S. Hennani, and H. Nebdi, "Theoretical introduction and generation method of a novel nondiffracting waves: Olver beams," *Optics and Photonics Journal*, Vol. 5, 234–246, 2015.
22. Gradshteyn, I. S. and I. M. Ryzhik, *Tables of Integrals Series and Products*, 5th edition, Academic Press, New York, 1994.